Third-order nonlinear femtosecond optical gating through highly scattering media

Maïmouna Bocoum[*]

Institut Langevin, ESPCI Paris, Université PSL, CNRS, 75005 Paris, France

Zhao Cheng,[†] Jaismeen Kaur,[‡] and Rodrigo Lopez-Martens[§]

Laboratoire d'Optique Appliquée, CNRS, Ecole Polytechnique, ENSTA Paris, Institut Polytechnique de Paris,
181 chemin de la Hunière et des Joncherettes, 91120 Palaiseau, France

Discriminating between ballistic and diffuse components of light propagating through highly scattering media is not only important for imaging purposes but also for investigating the fundamental diffusion properties of the medium itself. Massively developed to this end over the past 20 years, nonlinear temporal gating remains limited to $\sim 10^{-10}$ transmission factors. Here, we report nonlinear time-gated measurements of highly scattered femtosecond pulses with transmission factors as low as $\approx 10^{-12}$. Our approach is based on the third-order nonlinear cross-correlation of femtosecond pulses, a standard diagnostic used in high-power laser science, applied to the study of fundamental light scattering properties.

When an ultrashort light pulse propagates through a scattering medium, its intensity undergoes an exponential decrease with ballistic propagation quantified by the scattering coefficient μ_s. Simultaneously, a slower diffused component of light rises, withholding additional information about the medium. In a transmission configuration, temporal gating of the ballistic component may be exploited for shadow imaging [1] or to simply extract μ_s from the attenuation $e^{-\mu_s L}$ factor [2,3], where L is the length of the medium. In the highly scattering regime, where propagation is described by a diffusion equation [4], fitting the temporal shape of either the transmitted or reflected light at longer times ($\gg$ps) provides a measure of the diffusion coefficient $D = v_e/(3\mu'_s)$, where v_e is the energy velocity [5] and μ'_s the inverse of the transport mean free path [4]. Measuring both μ_s and μ'_s is crucial to fully characterize a scattering media as they are related by the relation $\mu'_s = \mu_s(1 - g)$, where g is the anisotropy which quantifies the directionality of the scattering process. Although direct measurements of μ'_s often rely on the use of coherent backscattering (CBS) techniques [6,7] or photonic Ohm-law static transmission [8], time gating methods may also be applied to the characterization of biological samples or scattering phantoms whenever the value of v_e is known [9,10]. The main advantage of temporal gating over CBS is its sensitivity to D over time as opposed to μ'_s only, hence the additional information it provides about the spatial or spectral behavior of the scatterers inside the medium. In the early 2000s, temporal gating was for instance used to demonstrate the transition from diffuse to localized propagation states when $\mu'_s \sim \lambda^{-1}$ [11], where λ designates the

wavelength of the scattered light. Although this interpretation has since been subject to debate and most likely attributable to fluorescence [12], temporal gating remains a powerful experimental tool for exploring deviations from classical diffusion behavior and their link to the mesoscopic topology of the scattering medium [13–16].

We often undermine how crucial the choice of temporal detection method is relative to the application or sample properties. Coherent gating either in the temporal [17,18] or spectral domains [15,19] has been extensively used to probe the temporal dynamics of multiply scattered light. The measured quantity, however, is not the averaged diffused intensity by the medium but rather its temporal (Green's function) [18] or spectral response (transfer function) [15,19] for one realization of disorder. Probing the diffusion properties of a given scattering medium therefore requires averaging over multiple realizations of disorder [1,15,20]. In addition, the bandwidth of the measured transfer function is limited by that of the illumination source [20], and the maximum measurable time window either by the excursion of the delay stage used for temporal measurements or by the resolution of the spectrometer in the case of spectral measurements. This limitation is extremely problematic because nonclassical propagation behavior such as localization effects [21–23] are expected for very long delays and low transmission factors. To circumvent this experimental difficulty, one must rely on incoherent temporal detection that is sensitive to the intensity of the scattered light.

Historically, such time-resolved experiments were based on streak camera gating [24–27], but the linear dynamic range of digital sensors makes it inadequate for temporal acquisitions with log variation in time. Single-photon counting detectors offer excellent sensitivity but feature limited temporal resolution, such that temporal traces have only been reported in the nanosecond range [9,11]. In a transmission measurement where the spreading of the incident pulse scales

---

[*]maimouna.bocoum@espci.fr

[†]zhao.cheng@ensta-paris.fr

[‡]jaismeen.kaur@ensta-paris.fr

[§]rodrigo.lopez-martens@ensta-paris.fr

with the Thouless time $\tau_l = L^2/D$ [28], the scope of investigation is therefore restricted to highly scattering phantoms such as solid powders [11,29], unresembling biological tissues or diluted phantoms, unless the measurement is performed in a (less precise) semi-infinite reflection configuration [9,30].

The 1990s witnessed the emergence of nonlinear temporal gating techniques with femtosecond laser pulses [2,3,31–33], combining both high temporal resolution and high dynamic detection range. Although techniques such as second-harmonic generation (SHG) gating [33] or optical Kerr gating (OKG) [2,3,31] are very efficient to probe complex media, the lowest transmission factor reported is $\sim 10^{-10}$ [2,34], which is still too high for characterizing fat emulsions in transmission. In this Letter, we show how third-harmonic generation (THG), a standard technique in high-power laser science with sensitivities of $\sim 10^{-12}$ or higher, can be used to characterize a highly scattering slab in transmission. Although comparable sensitivities have been reported, using state-or-the-art setups based on optical parametric amplification or even SHG in one case [35,36] that could in principle reach similar sensitivities, our approach offers immediate access to this record level of sensitivity using almost the highest dynamic range accessible today, all this using a commercially available device that anybody can buy and operate. We illustrate this by performing a simultaneous measurement of both the scattering coefficient μ_s and reduced scattering coefficient μ_s' of a fat emulsion in a transmission geometry.

THG cross-correlators were originally developed to diagnose unwanted pedestals, pre-pulses, or amplified spontaneous emission (ASE) on the picosecond-to-nanosecond timescale surrounding the peak of ultraintense femtosecond laser pulses [37–40], and can reach up to 10^{13} dynamic range in the near-IR (NIR) spectral region [39,41,42]. In our experiment, we use a commercial all-reflective third-order cross-correlator (Tundra, Ultrafast Innovations GmbH) featuring a 10^{12} dynamic detection range. A schematic representation of the cross-correlator setup is shown in Fig. 1(c). S-polarized 30 fs input pulses, centered at 790 nm, with 400 μJ energy, are sent into the device at a 1 kHz repetition rate. Each pulse is separated into a probe and a gate pulse with a 5:95% beam splitter. The 20 μJ probe pulse of ≈ 5 mm in diameter is attenuated using variable calibrated reflectivity mirrors (RA in Fig. 1) so as to keep the PMT response linear. The pulse is then sent through the scattering medium, located in between two long-range delay lines, while the gate pulse undergoes type-I SHG in a beta barium borate (BBO) crystal to generate a P-polarized SHG gate pulse centered at 2ω, where ω is the central laser frequency. The SHG gate pulse is filtered out from the residual NIR pulse using dichroic mirrors, converted back to S polarization with a periscope and mixed with the time-delayed S component of the scattered pulse in a type-I THG crystal to generate the cross-correlation signal at 3ω. The cross-correlation trace is obtained by recording the spatiospectrally filtered 3ω signal with a solar blind photomultiplier tube (PMT) as a function of delay between scattered and gate pulses, with a maximum delay of up to ± 2 ns and ~ 100 fs temporal resolution at best. Each data point is an average of 100 consecutive shots recorded in 100 fs time steps, except for the range spanning from -10 to $+10$ ps, where data are recorded in 10 fs time steps. A
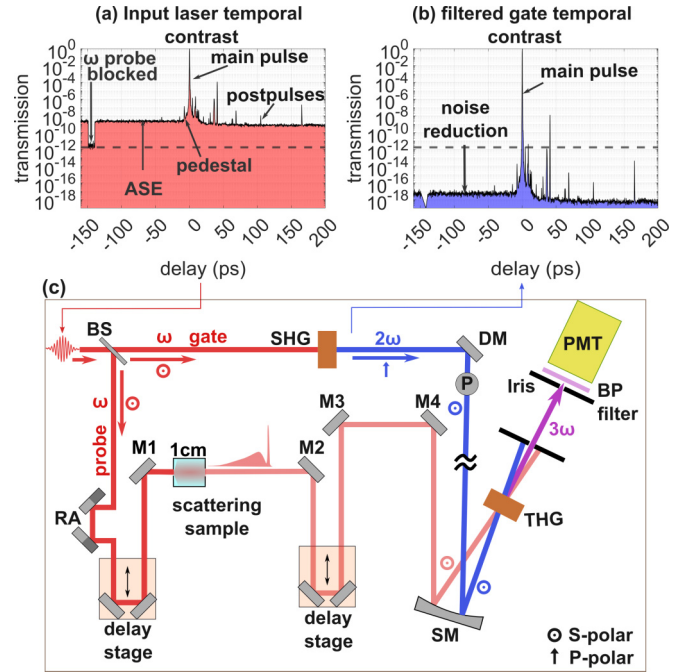

FIG. 1. (a) THG cross-correlation measurement of the input NIR laser pulse profile, normalized to its peak intensity. ASE: amplified spontaneous emission. (b) Calculated square root of the measured temporal NIR pulse profile (c) THG cross-correlator setup. M1, M2, M3, M4: silver mirrors. BS: beam splitter. RA: reflective attenuator set. DM: dichroic mirror. P: periscope. SHG: second-harmonic generation crystal. THG: third-harmonic generation crystal. SM: spherical focusing mirror. Retroreflectors are mounted on two high-stability delay stages. PMT: photomultiplier tube.

typical cross-correlation trace of the (unscattered) input laser pulse is shown in Fig. 1(a) over a 350 ps time window around the pulse peak. A detection noise floor of $\sim 10^{-12}$ can indeed be measured by blocking the ω probe arm at early times in the trace. The key to noise reduction in THG cross-correlators is the very low level of self-generated signal leaking from either arm of the optical setup into the 3ω detector [38,41].

To demonstrate the potential of a $\sim 10^{-12}$ sensitivity for the detection of diffused light, we characterized the scattering properties of a commercial intralipid-10% emulsion used in previous scattering experiments [43]. Fat emulsions are extensively used as light scattering models or as phantoms for biological applications [43,44]. The reason is an accessible price, low absorption ($\mu_a \ll \mu_s$), scalability of scattering properties with dilution, and the spherical shape of the fat droplets, which makes them easy to model using Mie theory. Despite this, measuring their scattering properties remains a challenge and different methods can yield significantly different results [45]. In particular, temporal gating characterization requires fulfilling the diffusion approximation, i.e., (i) $L\mu_s' \gg 1$, (ii) $\mu_a \ll \mu_s$, and (iii) $t \gg (v_e \mu_s')^{-1}$. Considering a short pulse incident on a fat emulsion slab modeled by a Dirac function in time, the average intensity I_d (W/cm^2) of the diffused component writes [4]

$$I_d(t) = E_{in} \frac{H(t)D}{d} \sum_{m=1}^{\infty} \frac{m\pi}{d} \sin\left(\frac{\pi m L}{d}\right) e^{-\frac{\pi^2 m^2 Dt}{L^2}} e^{-\mu_a ct}, \quad (1)$$
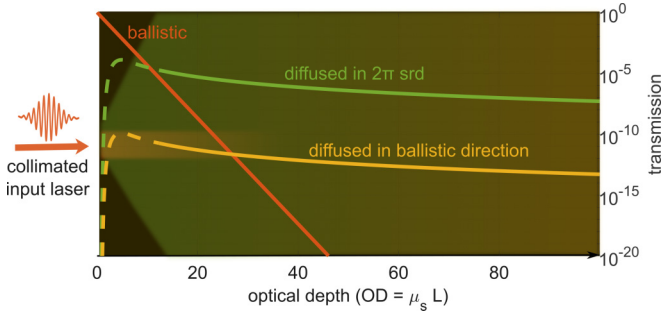
FIG. 2. Maximum transmission plotted as a function of L for the ballistic component (red curve) and the diffused light collected over 2π sr (green upper curve), or limited to $2\pi 10^{-6}$ sr in the ballistic direction (yellow lower curve) using a $\tau = 25$ fs temporal gate. Dashed lines indicate maximum transmission occurs at a time $t < 10(v_e\mu_s')^{-1}$, so as to outline the limited accuracy of Eq. (1). The scattering properties of the medium are set to $\mu_s = 20$ cm^{-1}, $\mu_a = 0$ cm^{-1}, and $g = 0.5$.

where $H(t)$ is the Heaviside function, t the time following the pulse arrival time on the slab, L the slab width, $d = L + z_0$, with z_0 as an adjustable parameter on the order of $z_0 \sim (\mu_s')^{-1}$, necessary to account for boundary conditions at the slab interface [4], and E_{in}(J/cm^2) the incident pulse fluence. We now define the transmission T_d as the ratio between detected and incident pulse fluence, over the gate time τ, the solid angle $\delta\Omega$, and a single polarization state, such that $T_d = \tau\delta\Omega I_d(t)/(4\pi E_{in})$. Recalling that for nonresonant scattering media, $v_e = c/n$, where c is the velocity of light in vacuum, and n the effective index of the medium [4], the maximum transmission evaluated from Eq. (1) occurs at $t \sim 0.09L^2/D$, and yields the scaling law

$$T_{d,max} \sim \frac{0.1\pi c\tau\delta\Omega}{n(1-g)^2\mu_s^2 L^3} \sim 1.4\frac{10^{-9}}{(1-g)^2 OD^2 L(cm)}, \quad (2)$$

where the numerical evaluation on the right-hand side is done for $\tau = 25$ fs, $n = 1.33$, and $\delta\Omega = 2\pi 10^{-6}$ sr, taken as a reference value from the SHG gating measurement reported in Ref. [34]. This simple scaling shows how crucial the detection sensitivity should be in order to explore large optical depths. In Fig. 2, we plot the maximum transmission of the diffused component obtained using Eq. (1) as we increase the propagation length L, for a given value $\mu_s = 20$ cm^{-1}, $\mu_a = 0$ cm^{-1}, and $g = 0.5$. The ballistic transmission in the same condition is plotted in red for comparison. In particular, by imposing $L\mu_s' \geqslant 10$ to satisfy the diffusion approximation, we have $T_{d,max} \lesssim 10^{-11}/L(cm)$, which is lower than the lowest transmission factor measured in Refs. [2,34], unless phantoms thinner than ~ 1 mm are used. In particular, in the past, the simultaneous measurement of both μ_s and μ_s' in fat emulsions was not done using nonlinear gated detection, but rather restricted to phantoms with high μ_s' and low L such as TiO$_2$ powders.

In our experiment, we measured the temporal transmission through a $L = 10$ mm long poly(methyl methacrylate) (PMMA) cuvette designed for absorption spectrometers (@plastibran) filled with intralipid-10% solution diluted in water at varying concentration $[c]$. The reference trace shown
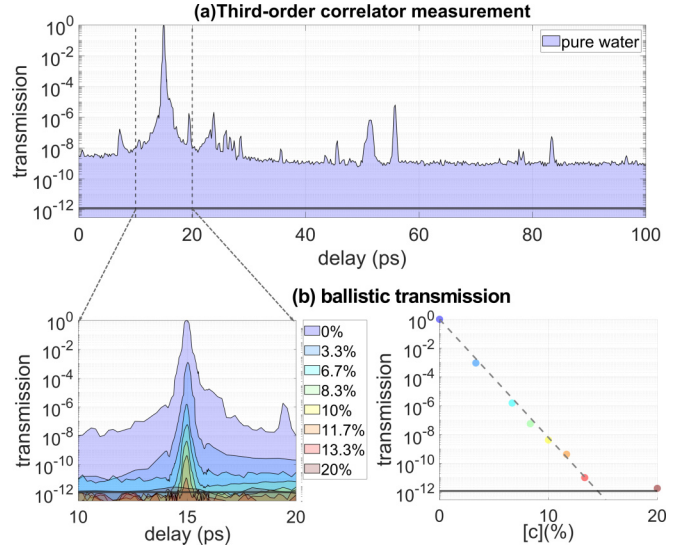

FIG. 3. (a) THG cross-correlation measurement through the cell filled with pure demineralized water and used for reference. (b) Same measurement with increasing intralipid-10% concentration $[c]$ (color coded) zoomed in over a 20 ps time window around the ballistic component centered at ~ 15 ps (left) and a linear fit of the peak value using $\mu_s = (189 \pm 10)[c]$ cm^{-1} (right).

in Fig 2(a) corresponds to a cuvette filled with only pure demineralized water and used for normalization. The ballistic peak is measured at a delay of $+15 \pm 0.2$ ps, corresponding to the propagation delay induced by the water-filled cuvette relative to air [see Fig. 1(a)]. Note that we expect a change in effective index limited to $\delta n \sim 4 \times 10^{-4}$ for the highest concentration of intralipid, which means a ballistic delay shift hardly resolvable with our detector. On the left-hand panel of Fig. 3(b), a zoom on the ballistic component is plotted for $[c] = 3.3\%$, 6.7%, 8.3%, 10%, 11.7%, and 20%, and the peak value is reported on the right-hand panel plot using the same color scale. A good fit of the ballistic attenuation is extracted from the $[c] = 13.3\%$ trace and represented by the black dotted line. We retrieve $\mu_s = (189 \pm 10)[c]$ cm^{-1}, where $0 \leqslant [c] \leqslant 1$ is the dimensionless diluted concentration of intralipid. This value is lower than $\mu_{s,th} = 281[c]$ cm^{-1} reported in Ref. [46] at 790 nm, but higher than $\mu_{s,th} = 100[c]$ cm^{-1} reported in Ref. [44]. Although the use of different brands or preparation methods could explain the discrepancy with values found in the literature [44], we believe our method to be more precise because it is based on temporal gating.

The value μ_s' is obtained by fitting the temporal profile at long times with Eq. (1), using the same trace used to measure μ_s. The effective index n is extrapolated from the relative percentage of water and soybean at a given concentration $[c]$ [44], $\tau = 25$ fs, and by manually adjusting the angle of collection to $\delta\Omega = 5.1\pi 10^{-6}$ sr, corresponding to a half collection angle of $\sim 0.13°$. We obtained the fit plotted in red in Fig. 4(c), where we retrieve $\mu_s' = (79 \pm 7)[c]$ cm^{-1}. Note that at this concentration, the diffusion approximation is verified since $\mu_s'L \gtrsim 10$. By fixing that value of μ_s', we superimposed the theoretical prediction with experimental data obtained for $[c] = 6.7\%$, 8.3%, and 20% in Figs. 4(a), 4(b) and 4(d), respectively. The slight departure from the theoretical fit
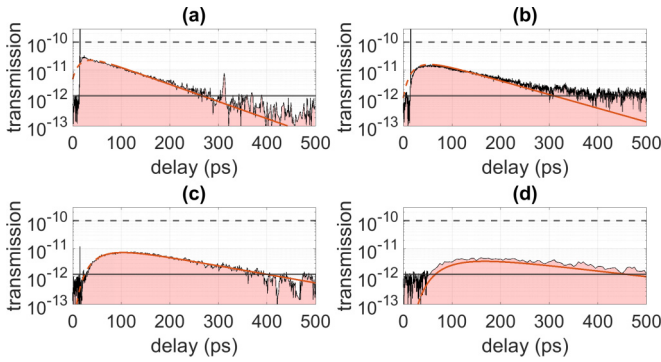
FIG. 4. THG cross-correlation traces obtained for (a) $[c] = 6.7\%$, (b) $[c] = 8.3\%$, (c) $[c] = 13.3\%$, and (d) $[c] = 20\%$. All red line fits are extracted from (c) providing $\mu'_s = (79 \pm 7)[c]$ cm^{-1} and based on Eq. (1) with $\tau = 25$ fs, $\delta\Omega = 5.1\pi\,10^{-6}$ sr. The horizontal solid and dotted gray lines correspond respectively to our detector noise level and the lowest reported in the literature [2,34].

observed in Figs. 4(a) and 4(b) corresponds to an error of up to 13% in the evaluation of μ'_s. This slope deviation may be attributed to error bars in the concentration calibration of our samples, or to a slight departure from the diffusion approximation, since in both cases, $\mu'_s L < 10$. In particular, the residual presence of ballistic postpulses at long delays [e.g.. the peak observed around $+310$ ps in Fig. 4(a)] indicates that we are not in a purely diffusive regime. The predicted temporal shape fits much better at $[c] = 20\%$ shown in Fig. 4(d), as we would expect. However, we do observe an unexpected $\sim 30\%$ higher transmission that cannot be explained by considering a variation in the average index of the medium. Measuring such features was clearly out of reach for the most sensitive nonlinear gating detection methods reported thus far [2,34], as indicated by the black dotted lines in Fig. 4. To ensure the reproducibility of our results, we repeated the measurement

multiple times over several days and got the same result to within 5% error. Finally, from the combined measurement of both μ_s and μ'_s, we estimate the anisotropic factor $g = 1 - \frac{\mu'_s}{\mu_s} = 0.58 \pm 0.08$. A theoretical value of $g_{th} = 0.64$ is predicted in Ref. [46] and $g_{th} = 0.32$ in Ref. [44] at 790 nm wavelength.

In conclusion, we used THG cross-correlation to perform a simultaneous measurement of both μ_s and μ'_s by measuring the ballistic transmission and long-time semilog variation of a short femtosecond NIR pulse transmitted through a scattering solution of $[c]$-diluted solution of intralipid-10% in water. We measured $\mu_s = (189 \pm 10)[c]$ cm^{-1} and $\mu'_s = (79 \pm 7)[c]$ cm^{-1}, from which we deduce $g = 0.58 \pm 0.08$ at 790 nm wavelength. Although intralipid is extensively used in scattering experiments and in the design of biological phantoms, we simultaneously measured both μ_s and μ'_s using nonlinear temporal gating. The reason for this is twofold: (i) Nonlinear temporal gating is highly restricted in an angular collection angle such that expected transmissions can easily be $\leqslant 10^{-10}$ for diffused light, and (ii) all detection systems used so far were limited in the dynamic range to $\sim 10^{10}$, making the characterization of the diffused light almost impossible. We have demonstrated how to overcome these challenges by implementing third-order nonlinear femtosecond temporal gating with a limit of detection of the order of $\sim 10^{-12}$, which is two orders of magnitude beyond the current state-of-the-art in terms of time-gated light scattering measurements. The sensitivity of most recent commercially available THG cross-correlators can reach up to $\sim 10^{-14}$ [47]. This record level of sensitivity could greatly facilitate the characterization of fat emulsion phantoms and opens the door to the exploration of diffusion dynamics that may deviate from classical predictions.

[1] M. R. Hee, J. A. Izatt, J. M. Jacobson, J. G. Fujimoto, and E. A. Swanson, Femtosecond transillumination optical coherence tomography, Opt. Lett. **18**, 950 (1993).

[2] J. Tong, Y. Yang, J. Si, W. Tan, F. Chen, W. Yi, and X. Hou, Measurements of the scattering coefficients of intralipid solutions by a femtosecond optical Kerr gate, Opt. Eng. **50**, 043607 (2011).

[3] L. Wang, X. Liang, P. Galland, P. Ho, and R. Alfano, True scattering coefficients of turbid matter measured by early-time gating, Opt. Lett. **20**, 913 (1995).

[4] R. Carminati and J. C. Schotland, *Principles of Scattering and Transport of Light* (Cambridge University Press, Cambridge, U.K., 2021).

[5] A. Lagendijk and B. A. Van Tiggelen, Resonant multiple scattering of light, Phys. Rep. **270**, 143 (1996).

[6] P. Wolf, G. Maret, E. Akkermans, and R. Maynard, Optical coherent backscattering by random media: An experimental study, J. Phys. France **49**, 63 (1988).

[7] U. Tricoli and R. Carminati, Modeling of full-field optical coherence tomography in scattering media, J. Opt. Soc. Am. A **36**, C122 (2019).

[8] R. Sapienza, P. D. García, J. Bertolotti, M. D. Martín, A. Blanco, L. Vina, C. López, and D. S. Wiersma, Observation of Resonant Behavior in the Energy Velocity of Diffused Light, Phys. Rev. Lett. **99**, 233902 (2007).

[9] S. J. Madsen, B. C. Wilson, M. S. Patterson, Y. D. Park, S. L. Jacques, and Y. Hefetz, Experimental tests of a simple diffusion model for the estimation of scattering and absorption coefficients of turbid media from time-resolved diffuse reflectance measurements, Appl. Opt. **31**, 3509 (1992).

[10] I. Bargigia, A. Tosi, A. B. Shehata, A. Della Frera, A. Farina, A. Bassi, P. Taroni, A. Dalla Mora, F. Zappa, R. Cubeddu *et al.*, Time-resolved diffuse optical spectroscopy up to 1700 nm by means of a time-gated InGaAs/InP single-photon avalanche diode, Appl. Spectrosc. **66**, 944 (2012).

[11] M. Störzer, P. Gross, C. M. Aegerter, and G. Maret, Observation of the Critical Regime Near Anderson Localization of Light, Phys. Rev. Lett. **96**, 063904 (2006).

[12] T. Sperling, L. Schertel, M. Ackermann, G. J. Aubry, C. M. Aegerter, and G. Maret, Can 3D light localization be reached in 'white paint'?, New J. Phys. **18**, 013039 (2016).

[13] M. P. van Albada, B. A. van Tiggelen, A. Lagendijk, and A. Tip, Speed of propagation of classical waves in strongly scattering media, Phys. Rev. Lett. **66**, 3132 (1991).

[14] K. Busch and C. M. Soukoulis, Transport Properties of Random Media: A New Effective Medium Theory, Phys. Rev. Lett. **75**, 3442 (1995).

[15] P. M. Johnson, A. Imhof, B. P. J. Bret, J. G. Rivas, and A. Lagendijk, Time-resolved pulse propagation in a strongly scattering material, Phys. Rev. E **68**, 016604 (2003).

[16] D. S. Wiersma, A. Muzzi, M. Colocci, and R. Righini, Time-resolved experiments on light diffusion in anisotropic random media, Phys. Rev. E **62**, 6681 (2000).

[17] L. A. Cobus, G. Maret, and A. Aubry, Crossover from renormalized to conventional diffusion near the three-dimensional Anderson localization transition for light, Phys. Rev. B **106**, 014208, (2022).

[18] A. Badon, G. Lerosey, A. C. Boccara, M. Fink, and A. Aubry, Retrieving Time-Dependent Green's Functions in Optics with Low-Coherence Interferometry, Phys. Rev. Lett. **114**, 023901 (2015).

[19] R. H. Kop and R. Sprik, Phase-sensitive interferometry with ultrashort optical pulses, Rev. Sci. Instrum. **66**, 5459 (1995).

[20] I. M. Vellekoop, P. Lodahl, and A. Lagendijk, Determination of the diffusion constant using phase-sensitive measurements, Phys. Rev. E **71**, 056604 (2005).

[21] S. John, Strong localization of photons in certain disordered dielectric superlattices, Phys. Rev. Lett. **58**, 2486 (1987).

[22] M. Segev, Y. Silberberg, and D. N. Christodoulides, Anderson localization of light, Nat. Photonics **7**, 197 (2013).

[23] T. Schwartz, G. Bartal, S. Fishman, and M. Segev, Transport and Anderson localization in disordered two-dimensional photonic lattices, Nature (London) **446**, 52 (2007).

[24] K. Yoo and R. Alfano, Time-resolved coherent and incoherent components of forward light scattering in random media, Opt. Lett. **15**, 320 (1990).

[25] P. P. Ho, P. Baldeck, K. Wong, K. Yoo, D. Lee, and R. Alfano, Time dynamics of photon migration in semiopaque random media, Appl. Opt. **28**, 2304 (1989).

[26] J. C. Hebden, R. A. Kruger, and K. Wong, Time resolved imaging through a highly scattering medium, Appl. Opt. **30**, 788 (1991).

[27] N. Bruce, F. Schmidt, J. Dainty, N. Barry, S. Hyde, and P. French, Investigation of the temporal spread of an ultrashort light pulse on transmission through a highly scattering medium, Appl. Opt. **34**, 5823 (1995).

[28] D. J. Thouless, Electrons in disordered systems and the theory of localization, Phys. Rep. **13**, 93 (1974).

[29] G. H. Watson, P. A. Fleury, and S. L. McCall, Searching for photon localization in the time domain, Phys. Rev. Lett. **58**, 945 (1987).

[30] M. S. Patterson, B. Chance, and B. C. Wilson, Time resolved reflectance and transmittance for the noninvasive measurement of tissue optical properties, Appl. Opt. **28**, 2331 (1989).

[31] L. Wang, P. Ho, C. Liu, G. Zhang, and R. Alfano, Ballistic 2-D imaging through scattering walls using an ultrafast optical Kerr gate, Science **253**, 769 (1991).

[32] S. Mujumdar and H. Ramachandran, Imaging through turbid media using polarization modulation: Dependence on scattering anisotropy, Opt. Commun. **241**, 1 (2004).

[33] C. Hauger, E. Baigar, T. Wilhelm, and W. Zinth, Time-resolved backscattering of femtosecond pulses from scattering media—an experimental and numerical investigation, Opt. Commun. **131**, 351 (1996).

[34] C. Calba, L. Méès, C. Rozé, and T. Girasole, Ultrashort pulse propagation through a strongly scattering medium: Simulation and experiments, J. Opt. Soc. Am. A **25**, 1541 (2008).

[35] E. J. Divall and I. N. Ross, High dynamic range contrast measurements by use of an optical parametric amplifier correlator, Opt. Lett. **29**, 2273 (2004).

[36] O. Konopolev, Y. Fisher, and D. Meyerhofer, Ultrahigh dynamic range measurement of high-contrast pulses using a second-order autocorrelator, LLE Rev. **75**, 159 (1998).

[37] K.-H. Hong, B. Hou, J. Nees, E. Power, and G. Mourou, Generation and measurement of $>10^8$ intensity contrast ratio in a relativistic kHz chirped-pulse amplified laser, Appl. Phys. B **81**, 447 (2005).

[38] S. Luan, M. Hutchinson, R. Smith, and F. Zhou, High dynamic range third-order correlation measurement of picosecond laser pulse shapes, Meas. Sci. Technol. **4**, 1426 (1993).

[39] J. Itatani, J. Faure, M. Nantel, G. Mourou, and S. Watanabe, Suppression of the amplified spontaneous emission in chirped-pulse-amplification lasers by clean high-energy seed-pulse injection, Opt. Commun. **148**, 70 (1998).

[40] K. Osvay, M. Csatári, I. Ross, A. Persson, and C.-G. Wahlström, On the temporal contrast of high intensity femtosecond laser pulses, Laser Part. Beams **23**, 327 (2005).

[41] V. Schanz, C. Brabetz, D. Posor, D. Reemts, M. Roth, and V. Bagnoud, High dynamic range, large temporal domain laser pulse measurement, Appl. Phys. B **125**, 61 (2019).

[42] J. Ma, P. Yuan, X. Ouyang, J. Wang, G. Xie, and L. Qian, Resolving ultrahigh-contrast ultrashort pulses with single-shot cross-correlator at the photon noise limit, arXiv:2102.12696.

[43] M. Bocoum, J. L. Gennisson, C. Venet, M. Chi, P. M. Petersen, A. A. Grabar, and F. Ramaz, Two-color interpolation of the absorption response for quantitative acousto-optic imaging, Opt. Lett. **43**, 399 (2018).

[44] R. Michels, F. Foschum, and A. Kienle, Optical properties of fat emulsions, Opt. Express **16**, 5907 (2008).

[45] A. Pifferi, A. Torricelli, A. Bassi, P. Taroni, R. Cubeddu, H. Wabnitz, D. Grosenick, M. Möller, R. Macdonald, J. Swartling *et al.*, Performance assessment of photon migration instruments: The MEDPHOT protocol, Appl. Opt. **44**, 2104 (2005).

[46] H. J. Van Staveren, C. J. Moes, J. van Marie, S. A. Prahl, and M. J. Van Gemert, Light scattering in lntralipid-10% in the wavelength range of 400–1100 nm, Appl. Opt. **30**, 4507 (1991).

[47] https://www.ultrafast-innovations.com/devices/TUNDRA. html.